European Journal of Plant Pathology **105:** 835–846, 1999.

Differentiation of *Rhizoctonia* AG-D isolates from turfgrass into subgroups I and II based on rDNA and RAPD analyses

Takeshi Toda[1], Mitsuro Hyakumachi[1,3,*], Haruhisa Suga[2], Koji Kageyama[1], Akemi Tanaka[4] and Toshikazu Tani[4]
[1]*Faculty of Agriculture,* [2]*Molecular Genetics Research Center, Gifu University, 1-1 Yanagido, Gifu 501-11, Japan;* [3]*Institute of Genetic Ecology, Tohoku University, Sendai 980-77, Japan;* [4]*Institute for Green Science, 3335-2 Showa, Nagao, Okawa, Kagawa 769-23, Japan;* [*]*Author for correspondence: Laboratory of Plant Disease Science, Faculty of Agriculture, Gifu University, 1-1 Yanagido, Gifu 501-11, Japan (Phone: +81(058)293-2847; Fax: +81(058)293-2847; E-mail: hyakumac@cc.gifu-u.ac.jp)*

Accepted 3 September 1999

Key words: turfgrass, binucleate, RFLP, ITS

Abstract

Binucleate *Rhizoctonia* anastomosis group (AG) D is the cause of rhizoctonia-patch and elephant-footprint diseases of zoysiagrass, and winter-patch disease of bentgrass. *Rhizoctonia* AG-D is also known as the causal pathogen of other diseases such as sharp-eye-spot of cereals, foot-rot of cereals and winter-stem-rot of mat rush. Isolates of AG-D have been divided into the two subgroups AG-D (I) and AG-D (II), based on the results of cultural characteristics and pathogenicity tests. Isolates obtained from zoysiagrass exhibiting symptoms of rhizoctonia-patch disease, from bentgrass with winter-patch disease, from wheat with foot-rot disease, and from mat rush with winter-stem-rot disease were reported to belong to subgroup AG-D (I). On the other hand, isolates obtained from zoysiagrass with elephant-footprint disease were assigned to subgroup AG-D (II). To confirm the existence of these two subgroups in AG-D, the genetic structure of AG-D isolates from turfgrass and other crops was compared. RFLP analysis of the ITS region from rDNA after digestion with the restriction enzymes *Eco*RI, *Hae*III, *Hha*I, *Hin*fI, and *Mbo*I separated AG-D isolates into two groups corresponding to AG-D (I) and AG-D (II). Furthermore, other AGs except AG-Q (AGs-A, Ba, Bb, C, E, F, G, I, K, L, O, P, and *R. solani* AG1-IC) did not have the same patterns that were seen for the two AG-D subgroups. AG-Q isolates from bentgrass showed the same patterns as AG-D (I). The results of the RAPD analysis also revealed the existence of two groups that corresponded to AG-D (I) and AG-D (II). These analyses revealed that *Rhizoctonia* AG-D isolates from turfgrass could be divided into two subgroups consistent with those based on cultural characteristics and pathogenicity. In addition, isolates of foot-rot disease of wheat and isolates of winter-stem-rot disease of mat rush whose cultural characteristics were the same as those of AG-D (I) also showed similar RFLP and RAPD patterns to those of AG-D (I) isolates from turfgrass.

Introduction

Fungi in binucleate *Rhizoctonia* anastomosis group D (*Rhizoctonia cerealis* = *Ceratobasidium* CAG-1 = *Rhizoctonia* AG-D) are soilborne fungal pathogens that cause foot-rot, root-rot, and damping-off diseases in several crop plants (Boerema and Verhoeven 1977; Ogoshi et al., 1979, 1983; Burpee, 1980; Burpee et al., 1980; Lipps and Herr, 1982; Uchino et al., 1983; Oniki et al., 1986b; Kataria and Hoffmann, 1988; Cubeta et al., 1991; Damaj et al., 1993). These pathogens also cause rhizoctonia-patch disease and elephant-footprint disease of Japanese and Manila zoysiagrasses (*Zoysia japonica* Steud and *Zoysia matorella* Err), and winter-patch disease of bentgrass (*Agrostis* spp.) (Oniki et al., 1986b; Tani, 1989; Tanpo et al., 1990). These three turfgrass diseases cause aesthetic damage to turfgrasses on golf courses. Rhizoctonia-patch and winter-patch

Table 1. Cultural characteristics and pathogenicity of *Rhizoctonia* AG-D isolates obtained from three turfgrass-, one wheat- and one mat rush-diseases

Disease	Host	Optimal temperature (°C)		Mycelial color	Sclerotial formation	Pathogenicity to		AG-D subgroup
		Hyphal growth	Causing disease			Zoysiagrass	Bentgrass	
Rhizoctonia-patch	Turfgrass	23	10	Brown	+	+	+	I
Winter-patch	Turfgrass	23	10	Brown	+	+	+	I
Elephant-footprint	Turfgrass	25	20	White to yellow	−	+	−	II
Foot-rot	Wheat	23	10	Brown	+	+	+	I
Winter-stem-rot	Mat rush	23	10	Brown	+	+	+	I

diseases commonly occur during the cool season in Japan, which is from December to May. On the other hand, elephant-footprint disease occurs during the hot season which is from June to September. Tanaka et al. (1994) suggested that isolates of AG-D obtained from turfgrasses exhibiting symptoms of these three diseases could be divided into two subgroups based on cultural characteristics and pathogenicity (Table 1). Tanaka et al. (1994) proposed that isolates from the rhizoctonia-patch and winter-patch diseases belong to subgroup AG-D (I), while the fungus causing elephant-footprint disease belongs to subgroup AG-D (II). From their cultural characteristics, isolates obtained from wheat with foot-rot disease and from mat rush with winter-stem-rot disease also belong to subgroup AG-D (I) (Table 1). In this study, the genetic structures of the two subgroups of *Rhizoctonia* AG-D were compared by RFLP analysis of the ITS region from rDNA and by RAPD analysis, to test whether these two subgroups are genetically distinct.

Materials and methods

Isolates

Seventy-nine isolates of *Rhizcotonia* spp. were used in this study. The origins of these isolates are listed in Tables 2 and 3. Twenty-one isolates were obtained from zoysiagrass exhibiting symptoms of elephant-footprint disease, twelve from zoysiagrass with rhizoctonia-patch disease, and seventeen from bentgrass with winter-patch disease. Two isolates obtained from wheat (*Triticum aestivum* L.) with foot-rot disease (Takamatsu, 1989) and three from mat rush (*Juncus decipiens* Nakai) with winter-stem-rot disease (Ikata and Yoshida, 1940; Matsuoka, 1959) were also used. Moreover, other binucleate isolates of AGs-A, Ba, Bb, C, E, F, G, I, K, L, O, P, Q (Ogoshi et al., 1978; Oniki et al., 1986a), and one isolate of *Rhizoctonia solani* AG1-IC (Hyakumachi and Sumino, 1984) were also used for comparison. All isolates were maintained on potato dextrose agar (PDA) in test tube slants at 25 °C.

Hyphal anastomosis

Isolates used for hyphal anastomosis reactions are listed in Tables 2 and 3. The methods for the microscopical observation of hyphal anastomoses within and between isolates of the two subgroups of AG-D or between the isolates of AG-D and other AGs were done as described by Ogoshi (1976). The isolates were grown on PDA for 2–3 days at 25 °C. Mycelial plugs of 3 mm diameter taken from the advancing margin of the pure culture of each isolate were paired 3–4 cm apart, on 2% water agar (WA), in a 9 cm petri dish, and allowed to grow at 25 °C. After 2 days, the overlapping portion of hyphae which was growing on WA was transferred to a slide, stained with 0.1% cotton blue in lactophenol, and observed for hyphal fusion at 100× magnification. Percentage fusion frequency was determined using the equation: $A(100)/B$, where A is the sum of fusion points, and B is the sum of contact points in 15 microscopic fields. The type of hyphal anastomosis reactions categorized by Carling and Leiner (1987) was determined by observation at 400× magnification.

DNA extraction

Seventy-two isolates used for DNA extraction are listed in Tables 2 and 3. These isolates were cultured in 10 ml of potato dextrose broth (PDB) at 25 °C for seven days. After incubation, the mycelial mat was harvested by filtration and stored at −80 °C until use. Total genomic DNA was extracted by

Table 2. Rhizoctonia AG-D isolates used in this study

Working number	HA[a]	ITS[b]	RAPD[c]	Isolate name	Disease	Subgroup	Host	Origin
R1	+	+	+	SN16	Rhizoctonia-patch	I	Zoysiagrass	Chiba
R2		+	+	TG-M-2	Rhizoctonia-patch	I	Zoysiagrass	Kagawa
R3	+	+	+	TG-SDS-1	Rhizoctonia-patch	I	Zoysiagrass	Kagawa
R4	+	+	+	B1-2	Rhizoctonia-patch	I	Zoysiagrass	—[d]
R5	+	+	+	T-9H-5	Rhizoctonia-patch	I	Zoysiagrass	Mie
R6		+	+	YC-SDS-1	Rhizoctonia-patch	I	Zoysiagrass	Mie
R7		+	+	ST-SDS-1	Rhizoctonia-patch	I	Zoysiagrass	Kagawa
R8	+	+		HR-12-1	Rhizoctonia-patch	I	Zoysiagrass	Shiga
R9	+			BrG-SDS-1	Rhizoctonia-patch	I	Zoysiagrass	Yamanashi
R10	+			SD-SDS-1	Rhizoctonia-patch	I	Zoysiagrass	Kagawa
R11	+			IZ-SDS-1	Rhizoctonia-patch	I	Zoysiagrass	Shimane
R12		+		CY-SDS-1	Rhizoctonia-patch	I	Zoysiagrass	Hiroshima
W1	+	+	+	WG1B	Winter-patch	I	Bentgrass	Kagawa
W2	+	+	+	AO-S-1A	Winter-patch	I	Bentgrass	Miyazaki
W3	+	+	+	WT-G	Winter-patch	I	Bentgrass	Hyogo
W4	+	+	+	MS-S-A2	Winter-patch	I	Bentgrass	—
W5			+	RF-WP-1	Winter-patch	I	Bentgrass	Miyagi
W6		+	+	KF-1	Winter-patch	I	Bentgrass	Fukuoka
W7		+	+	ST-WP-3	Winter-patch	I	Bentgrass	Kagawa
W8		+		WR2C	Winter-patch	I	Bentgrass	Kagawa
W9	+	+		YC-WP-3	Winter-patch	I	Bentgrass	Mie
W10		+		KuM-WP-2	Winter-patch	I	Bentgrass	Ehime
W11	+	+		BIG-WP-2	Winter-patch	I	Bentgrass	Yamagata
W12		+		CS-WP-2	Winter-patch	I	Bentgrass	Kumamoto
W13		+		ST-WP-2	Winter-patch	I	Bentgrass	Kagawa
W14		+		AYu-WP-1	Winter-patch	I	Bentgrass	Kagawa
W15		+		BrG-WP-2	Winter-patch	I	Bentgrass	Yamanashi
W16	+			OK-WP-2	Winter-patch	I	Bentgrass	Okayama
W17		+		WK-WP-3	Winter-patch	I	Bentgrass	Yamaguchi
E1	+	+	+	UN-3-2	Elephant-footprint	II	Zoysiagrass	Kagoshima
E2	+	+	+	TG9R	Elephant-footprint	II	Zoysiagrass	Kagawa
E3	+	+	+	SD-W4-5	Elephant-footprint	II	Zoysiagrass	Kagawa
E4		+	+	KT-1-1	Elephant-footprint	II	Zoysiagrass	Kagawa
E5		+	+	TG13R	Elephant-footprint	II	Zoysiagrass	Kagawa
E6	+	+	+	OK-EF-1	Elephant-footprint	II	Zoysiagrass	Okayama
E7	+	+	+	MW-EF-1	Elephant-footprint	II	Zoysiagrass	Yamaguchi
E8		+	+	MW-EF-2	Elephant-footprint	II	Zoysiagrass	Yamaguchi
E9	+	+		WK-EF-1	Elephant-footprint	II	Zoysiagrass	Yamaguchi
E10		+		ST-EF-1	Elephant-footprint	II	Zoysiagrass	Kagawa
E11	+	+		YC-EF-1	Elephant-footprint	II	Zoysiagrass	Mie
E12		+		YG-EF-1	Elephant-footprint	II	Zoysiagrass	Yamagata
E13		+		SB-EF-2	Elephant-footprint	II	Zoysiagrass	Chiba
E14	+	+		CH-EF-1	Elephant-footprint	II	Zoysiagrass	Aichi
E15		+		HR-EF-2	Elephant-footprint	II	Zoysiagrass	Shiga
E16		+		Oak-EF-1	Elephant-footprint	II	Zoysiagrass	Okayama
E17		+		WK-EF-3	Elephant-footprint	II	Zoysiagrass	Yamaguchi
E18		+		MW-EF-3	Elephant-footprint	II	Zoysiagrass	Yamaguchi
E19		+		ST-EF-2	Elephant-footprint	II	Zoysiagrass	Kagawa
E20		+		SD-EF-1	Elephant-footprint	II	Zoysiagrass	Kagawa
E21		+		KM-EF-1	Elephant-footprint	II	Zoysiagrass	Ehime
F1	+	+	+	W-12 (ATCC76318)	Foot-rot	I	Wheat	Hokkaido

Table 2. Continued

Working number	HA[a]	ITS[b]	RAPD[c]	Isolate name	Disease	Subgroup	Host	Origin
F2	+	+	+	C-60	Foot-rot	I	Wheat	—
M1	+			C-27	Winter-stem-rot	I	Mat rush	Fukuoka
M2		+		C-58	Winter-stem-rot	I	Mat rush	Fukuoka
M3	+	+	+	C-160	Winter-stem-rot	I	Mat rush	—

[a]Used for hyphal anastomosis observation.
[b]Used for RFLP analysis of ITS from rDNA.
[c]Used for RAPD analysis.
[d]Unknown.

Table 3. Rhizoctonia other than AG-D isolates used in this study

Working number	HA[a]	ITS[b]	RAPD[c]	Isolate name	Group	Host	Origin
A1	+	+		YS-10-1	AG-A	—[d]	—
A2		+		YS-6-4-2A	AG-A	—	—
Ba1	+	+	+	C-314	AG-Ba	—	—
Ba2	+	+		C-484	AG-Ba	*Oryza sativa* L.	Fukuoka
Bb1	+	+		C-455	AG-Bb	*Oryza sativa* L.	Fukuoka
Bb2	+	+		C-350	AG-Bb	—	—
C1	+	+		706	AG-C	*Dactylis glomerata* L.	Hokkaido
C2	+	+		N462	AG-C	*Dactylis glomerata* L.	—
E1	+	+		TMA1-1	AG-E	Soil	Hokkaido
E2	+	+		F-18	AG-E	*Linum usitatissimum* L.	Hokkaido
E3	+			RH155	AG-E	*Dactylis glomerata* L.	—
F1	+	+		AH-6	AG-F	*Arachis hypogaea* L.	Chiba
F2	+			S1R-1	AG-F	—	—
G1	+	+	+	AH-9	AG-G	*Arachis hypogaea* L.	Chiba
G2	+	+		HAK1-1	AG-G	Soil	Hokkaido
I1	+	+		AV-2	AG-I	*Artemisia*	Tokyo
I2	+	+		614	AG-I	*Dactylis glomesata* L.	—
K1	+	+		AC-1	AG-K	*Allium cepa* L.	Hokkaido
L1	+	+		—	AG-L	—	—
O1	+	+		O3	AG-O	—	—
P1		+		C-578	AG-P	*Thea sinensis* L.	Shizuoka
Q1	+	+		RK-2	AG-Q	*Agrostis* (bentgrass)	—
Q2		+		RK-3	AG-Q	*Agrostis* (bentgrass)	—
1-IC	+	+	+	P-1	*R. solani* AG1-IC	*Beta vulgaris* L.	Hokkaido

[a]Used for hyphal anastomosis observation.
[b]Used for RFLP analysis of ITS from rDNA.
[c]Used for RAPD analysis.
[d]Unknown.

following a method modified from Yoder (1988). Frozen mycelia were ground, suspended in extraction buffer (10 mM Tris-HCl pH 7.5, 100 mM EDTA, 0.5% sodium dodecyl sulphate (SDS) and 100 mM LiCl) and heated at 50 °C for 15 min. The supernatant obtained by centrifugation (15,000 rpm) was extracted with phenol–chloroform–isoamyl alcohol (25 : 24 : 1). The DNA was precipitated with isopropyl alcohol, rinsed with 70% ethanol and redissolved in a 50 µl volume of TE buffer (10 mM Tris-HCl, pH 7.5, 1 mM EDTA). After treatment with 10 µg RNase A (Sigma Chemical, USA) at 37 °C for 1 h, the DNA was extracted sequentially with Tris-saturated phenol, phenol–chloroform–isoamyl alcohol, chloroform–isoamyl alcohol (24 : 1) and diethyl ether. Isopropyl alcohol was added to the resulting solution and the

mixture was placed on ice for 10 min. The DNA precipitate collected by centrifugation was washed with 70% ethanol and dissolved in 50 µl of TE buffer.

PCR of the ITS region

Amplification reactions were carried out for fungal DNA of 71 isolates (Tables 2 and 3). The reaction mixture consisted of a 50 µl volume containing 100 µM each of dATP, dCTP, dGTP, and dTTP, 50 pmol each of the oligonucleotide primers ITS1 and ITS4 (Rikaken, Japan), 10 mM Tris-HCl, pH 8.3, 50 mM KCl, 1.5 mM $MgCl_2$, and 1.25 units *Taq* polymerase (Takara Shuzo, Japan). ITS1 and ITS4 are designed for the amplification of the ITS region from rDNA (White et al., 1990). The sequences of ITS1 and ITS4 are listed in Table 4. The reaction mixture was overlaid with mineral oil prior to PCR amplification. A DNA thermal cycler (The Perkin Elmer Cetus, USA) was programmed for 3 min at 94 °C, followed by 30 cycles of 1 min at 94 °C, 1 min at 59 °C, 1 min at 72 °C, and 7 min at 72 °C. After extraction with chloroform, the amplification products were separated by electrophoresis on 1.5% agarose gels (Takara Shuzo, Japan) in TBE buffer. The gels were stained with ethidium bromide (EB), and the DNA was visualized under UV trans-illumination.

Restriction enzyme digestion of the ITS region from rDNA

Amplified products of isolates used for ITS-PCR were precipitated in 3 M sodium acetate and 99.5% ethanol at −80 °C for 30 min, washed in 70% ethanol, dried under vacuum, and resuspended in 50 µl of TE buffer. The ITS region from rDNA of each isolate was digested separately, under conditions recommended by the manufacturer (Takara Shuzo, Japan), with seven restriction enzymes: *Eco*RI, *Hae*III, *Hha*I, *Hin*fI, *Mbo*I, *Pst*I, and *Xba*I. The restriction fragments were separated by electrophoresis on 2% NuSieve agarose gels (FMC BioProducts, USA).

Table 4. Sequence of primers used in the analysis of *Rhizoctonia* AG-D isolates

Primer name	Sequence
ITS1	5′-TCCGTAGGTGAACCTGCGC-3′
ITS4	5′-TCCTCCGCTTATTGATATGC-3′
P14	5′-CCACAGCACG-3′
R28	5′-ATGGATCCGC-3′
RC09	5′-GATAACGCAC-3′
A01	5′-TGCACTACAACA-3′
A07	5′-TGCCTCGCACCA-3′
A08	5′-GCCCCGTTAGCA-3′
A09	5′-CCGCAGTTAGAT-3′
R1	5′-GTCCATTCAGTCGGTGCT-3′

RAPD analysis

Amplification reactions were carried out using 28 isolates. These isolates are listed in Tables 2 and 3. Except for the primers, the reaction mixture was the same as that used for the amplification of the ITS region from rDNA. The primers used for the RAPD analysis were P14, R28, RC09, R1, A01, A07, A08, and A09 (Rikaken, Japan). The sequences of the RAPD primers are listed in Table 4. Reaction mixtures were overlaid with mineral oil prior to PCR amplification. The DNA thermal cycler was programmed for 2 min at 94 °C, followed by 40 cycles of 1 min at 94 °C, 1 min at 35 °C, 3 min at 72 °C, and with a final extension of 7 min at 72 °C. After extraction with chloroform, the amplification products were separated by electrophoresis on 1.5% agarose gels (Takara Shuzo, Japan) in TBE buffer. The gels were stained with EB, and the DNA was visualized under UV trans-illumination. The banding patterns of the DNA were estimated visually. A dendrogram was constructed from the results of the cluster analysis generated by similarity coefficients using the unweighted pair group method with arithmetic average (UPGMA)(Sneath and Sokal, 1973). The similarity coefficient F between two strains was detected by the formula of $F = 2N_{XY}/N_X + N_Y$, where N_{XY} is the number of common fragments between the two isolates, and N_X and N_Y, are the number of fragments in isolates X and Y, respectively. A dendrogram was also constructed from a bootstrap analysis. Binary data were taken from the banding patterns of the DNA and used for phylogenetic analysis. Maximum parsimony trees were produced using the heuristic method of PAUP 3.1.1 (Swofford, 1993). Clade stability was assessed with 100 bootstrap replications.

Results

Hyphal anastomosis

Hyphae of the AG-D isolates fused within and between the two subgroups, but failed to fuse with hyphae of *R. solani* AG1-IC and other binucleate *Rhizoctonia*

AGs, except AG-Q. A C2 reaction with both wall and membrane fusion and death of anastomosing cells was always observed in pairings made within and between the two subgroups of AG-D isolates, and between AG-D and AG-Q isolates. Within the two subgroups, hyphal anastomosis frequencies were 42.2 ± 1.7 (39.7–48.2%) for AG-D (I), and 46.8 ± 4.3 (42.5–51.1%) for AG-D (II). Anastomosis frequencies between subgroups were 44.7 ± 4.3 (30.5–48.4%). The two subgroups were not distinguishable by hyphal anastomosis frequency, and there was no difference in anastomosis frequencies within and among isolates causing the five different diseases and of AG-Q. For example, anastomosis frequencies within the isolates causing each disease were 40.9% ± 1.2 for rhizoctonia-patch, 42% ± 4.5 for winter-patch, 44.8% ± 3.4 for foot-rot, 43.5% ± 2.2 for winter-stem-rot, and 46.8% ± 4.3 for elephant-footprint. When isolates causing elephant-footprint disease were tested against the other isolates, the following anastomosis frequencies were found: 43.9% ± 3.0 with rhizoctonia-patch, 44.4% ± 4.4 with winter-patch, 45.8% ± 3.9 with foot-rot, 45.2% ± 3.8 with winter-stem-rot, and 43.4% ± 4.7 with AG-Q. There was no statistically significant difference in the means as determined by Duncan's multiple range test.

RFLP analysis of the ITS region from rDNA

The primers ITS1 and ITS4 gave a product of the ITS region from rDNA from all binucleate *Rhizoctonia* isolates. The DNA fragments differed for restriction digest patterns generated by the enzymes *Eco*RI, *Hae*III, *Hha*I, *Hin*fI, and *Mbo*I. However, the PCR-products were not cleaved by *Pst*I and *Xba*I. The length of PCR-products and restriction fragments were the same within each subgroup of AG-D and with isolates of the other AGs. Representative isolates of each AG are listed in Table 5. The *Eco*RI-digested products of all isolates had one restriction site and showed two fragments of different lengths. *Hha*I digestion also indicated that all AGs, except for AG-Bb, had one restriction site and showed two different-sized fragments. AG-Bb had two restriction sites and showed three fragments. *Hae*III, *Hin*f I and *Mbo*I digestion showed a variety of polymorphisms among all AGs. *Hin*f I and *Mbo*I digestion patterns are shown in Figure 1. AG-D showed two restriction fragment patterns for these five endonucleases. One pattern was composed of isolates from rhizoctonia-patch and winter-patch, which belong to subgroup AG-D (I); isolates causing foot-rot and winter-stem-rot were also included in this pattern. Another pattern was composed of isolates from elephant-footprint, which belong to AG-D (II). No other AGs except AG-Q had the same restriction patterns as AG-D (I) and AG-D (II). These results indicated that two subgroups of AG-D can be distinguished based on restriction digest patterns generated by these five enzymes. AG-Q showed the same patterns as AG-D (I).

Table 5. Restriction fragment sizes (base pairs) of the representative isolates of *Rhizoctonia* spp. after digestion of the ITS region from rDNA with five endonucleases[a]

AG	Working number	ITS	*Eco*RI	*Hae*III	*Hha*I	*Hin*f I	*Mbo*I
D(I)	R1	740	380,360	540,120,80	390,350	300,130,110,60	260,260,130,90
D(II)	E1	740	390,350	540,130,70	380,360	260,190,150,14	250,180,140,90
A	A1	720	390,330	580,100,40	390,330	280,230,130,80	230,210,130
Ba	Ba1	730	400,330	450,130,110	365,365	400,180,150	220,200,130,70
Bb	Bb1	810	440,370	650,120,60	405,405	420,320,70	260,260,130,70
C	C1	730	390,340	540,120,70	400,270,60	280,210,140	260,250,140,80
E	E1	740	390,350	580,110,50	380,360	390,350	260,260,140,80
F	F1	680	360,320	400,140,100,40	340,300,40	330,230,120	230,210,130,110
G	G1	710	390,320	550,120,50	355,355	380,330	260,240,150,60
I	I1	710	380,320	550,110,60	370,340	320,210,120,60	230,190,140,80,70
K	K1	740	400,340	470,100,100,70	370,370	390,290,60	270,250,150,70
L	L1	720	380,340	540,120,60	360,360	390,330	260,230,140,70
O	O1	720	390,330	320,120,120,60	360,360	340,280	260,240,140,80
P	P1	760	390,370	620,110,30	400,360	390,190,180	270,250,160,80
Q	Q1	740	380,360	540,120,80	390,350	300,130,110,60	260,260,130,90
IC	1-IC	690	370,320	400,130,100,60	360,330	360,330	250,240,140,60

[a]List of the representative isolates of *Rhizoctonia* spp. used in this experiment are shown in Tables 2 and 3.

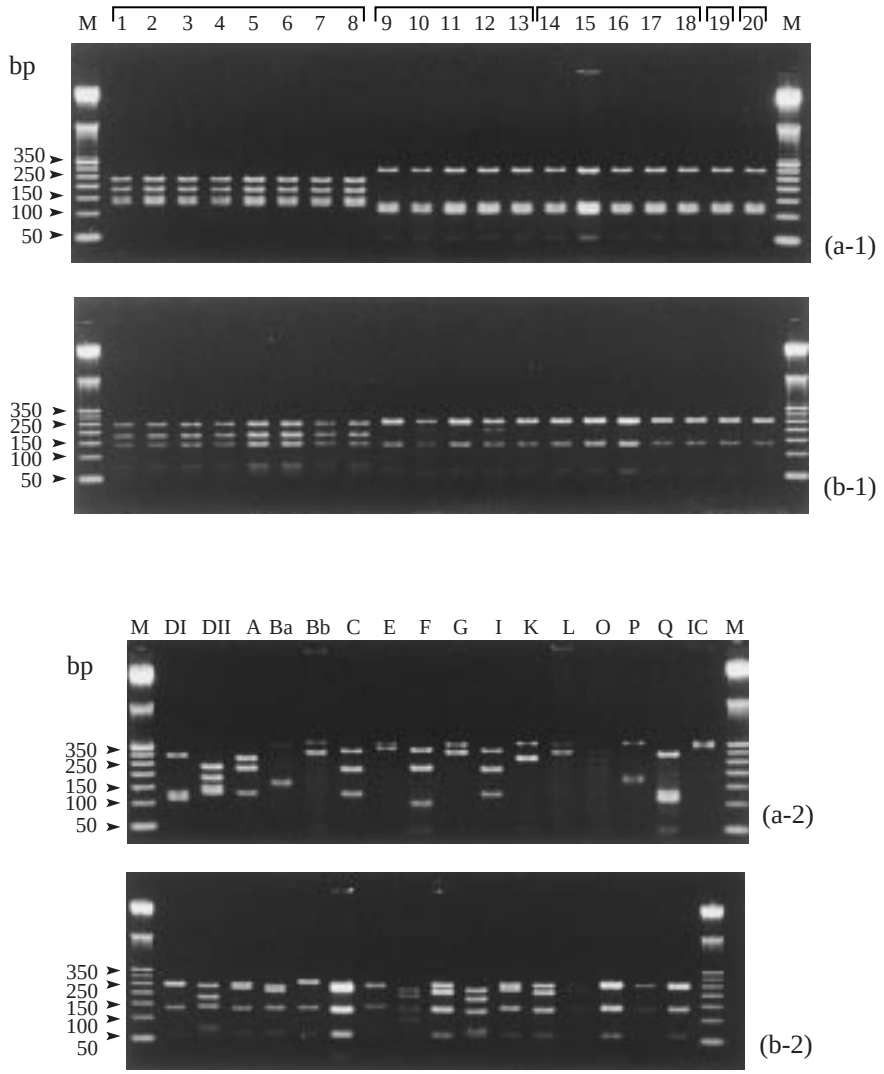

Figure 1. Agarose gels showing DNA restriction digest patterns of the rDNA-ITS region of *Rhizoctonia* isolates causing various diseases using endonucleases *Hin*f I (a-1, a-2) and *Mbo* I (b-1, b-2): Lanes 1–8, isolates (working number) E1, E2, E6, E7, E11, E13, E14 and E15 causing elephant-footprint; Lanes 9–13, isolates R1, R2, R5, R7 and R8 causing rhizoctonia-patch; Lanes 14–18, isolates W1, W2, W3, W5 and W6 causing winter-patch; Lane 19, isolate F1 causing foot-rot; Lane 20, isolate M3 from winter-stem-rot; Lanes DI, DII, A, Ba, Bb, C, E, F, G, I, K, L, O, P, Q and IC are representative isolates of the various groups and subgroups, and are working numbers R1, E2, Ba1, Bb1, C1, E1, F1, G1, I1, K1, L1, O1, P1, Q1, and 1-IC, respectively.

RAPD analysis

RAPD-PCR using 28 isolates was performed with eight primers that gave multiple PCR products. Isolates from each AG had identical banding patterns using all eight primers (data not shown). Representative banding patterns for isolates from AG-D and three other AGs (AG-Ba, G, and *R. solani* AG1-IC) using three primers (P14, R1 and A08) are shown in Figure 2. In isolates of AG-D, banding patterns obtained using the individual primers were clearly divided into two types. One type was composed of isolates causing rhizoctonia-patch and winter-patch diseases, which belong to subgroup AG-D (I); isolates causing foot-rot and winter-stem-rot diseases, which also belong to AG-D (I), were also included in this type. Another type consisted of isolates

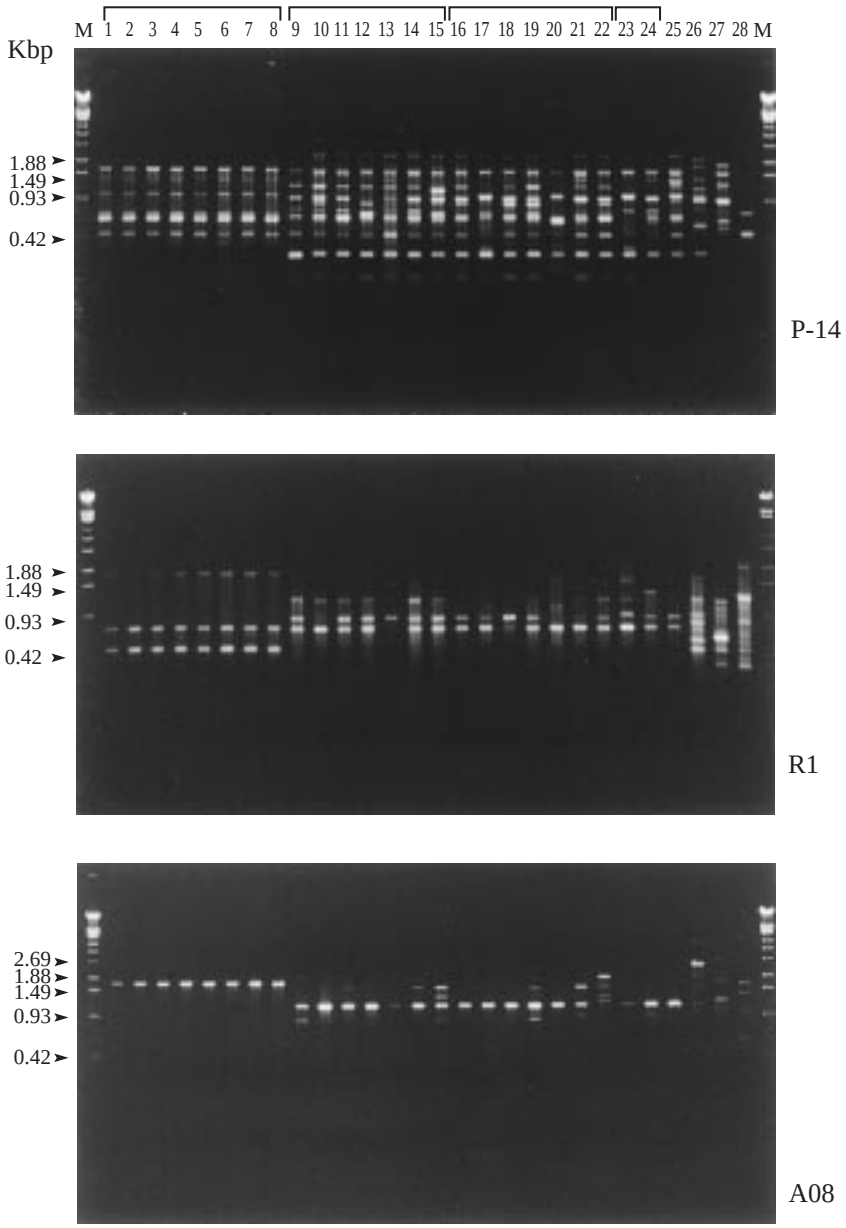

Figure 2. Random amplified polymorphic DNA (RAPD) banding patterns using primers P14, R1 and A08 of *Rhizoctonia* isolates causing various diseases: Lanes 1–8, isolates E1, E2, E4, E5, E6, E7 and E8 causing elephant-footprint; Lanes 9–15, isolates R1, R2, R3, R4, R5, R6 and R7 causing rhizoctonia-patch; Lanes 16–22, isolates W1, W2, W3, W4, W5, W6 and W7 causing winter-patch; Lanes 23–24, isolates F1 and F2 causing foot-rot; Lane 25, isolate M3 causing winter-stem-rot; Lane 26, isolate AG-Ba1; Lane 27, isolate AG-G1; and Lane 28, *R. solani* AG1-IC isolate.

from elephant-footprint disease, which belong to AG-D (II). The total number of bands from 28 isolates using the eight primers was 175. A dendrogram constructed using UPGMA was made from the data of these 28 isolates using all eight primers (Figure 3), and showed that AG-D isolates were separated into two clusters based on a similarity coefficient of 0.21. Isolates from rhizoctonia-patch, winter-patch, foot-rot, and winter-stem-rot formed one cluster with a minimum similarity coefficient of 0.57, and isolates from

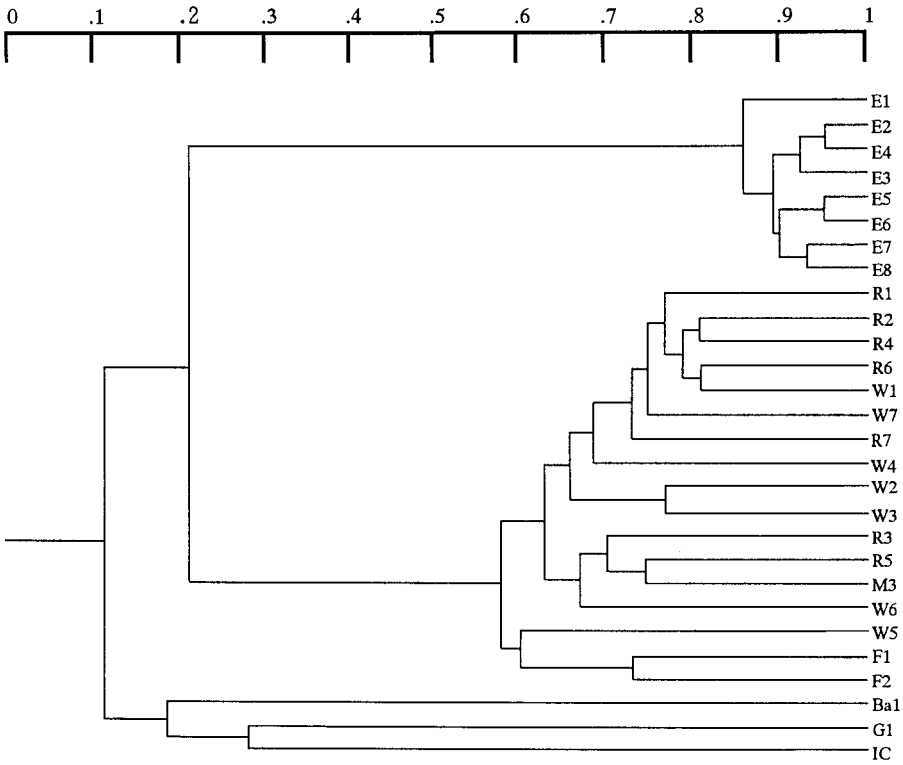

Figure 3. Dendrogram obtained from RAPD analysis showing different levels of genetic relatedness among *Rhizoctonia* binucleate AG-D subgroups (I) and (II), AG-Ba and AG-G isolates. The dendrogram was constructed from the similarity coefficient of UPGMA. For identification see Tables 2 and 3.

elephant-footprint formed another cluster with a minimum similarity coefficient of 0.86. The mean similarity coefficient between AG-D isolates and those in the other AGs was 0.11. RAPD analyses clearly indicated that AG-D could be divided into two subgroups representing AG-D (I) and AG-D (II). A phylogenetic tree constructed using PAUP 3.1.1. from the same banding data also showed that AG-D isolates were separated into two clusters corresponding to subgroups I and II (Figure 4). Isolates from rhizoctonia-patch, winter-patch, foot-rot, and winter-stem-rot formed one cluster 98 times out of 100 bootstrap replicates. Isolates of elephant footprint formed a cluster separate from the cluster for the other diseases for all 100 bootstrap replicates.

Discussion

Ribosomal RNA genes are known to be conserved, and so sequence component analyses of these genes are phylogenetically and taxonomically informative (Bruns et al., 1991). Recently, analysis of ribosomal DNA has been used for classification of *Rhizoctonia* species (Jabaji-Hare et al., 1990; Vilgalys and Gonzalez, 1990; Liu and Sinclair, 1992, 1993; Liu et al., 1993, 1995; Balali et al., 1996). Also, the delimitation of binucleate *Rhizoctonia* AGs has been supported by DNA analyses (Cubeta et al., 1991; Damaj et al., 1993). In addition, some reports have indicated that RFLP analysis of the ITS region from rDNA and RAPD analysis could be used for inter- or intra-group differentiation of *Rhizoctonia* spp. (Liu and Sinclair, 1992, 1993; Duncan et al., 1993; Boysen et al., 1996; Keijer et al., 1996; Yang and Kharbanda, 1996; Schneider et al., 1997). The present study has also demonstrated that the two subgroups of AG-D are clearly distinguishable from each other. Restriction digest patterns of the ITS region from rDNA by the enzymes *Eco*RI, *Hae*III, *Hha*I, *Hin*fI, and *Mbo*I clearly distinguished two subgroups of AG-D, which were different from other binucleate groups except AG-Q. Hyphae of AG-Q isolates

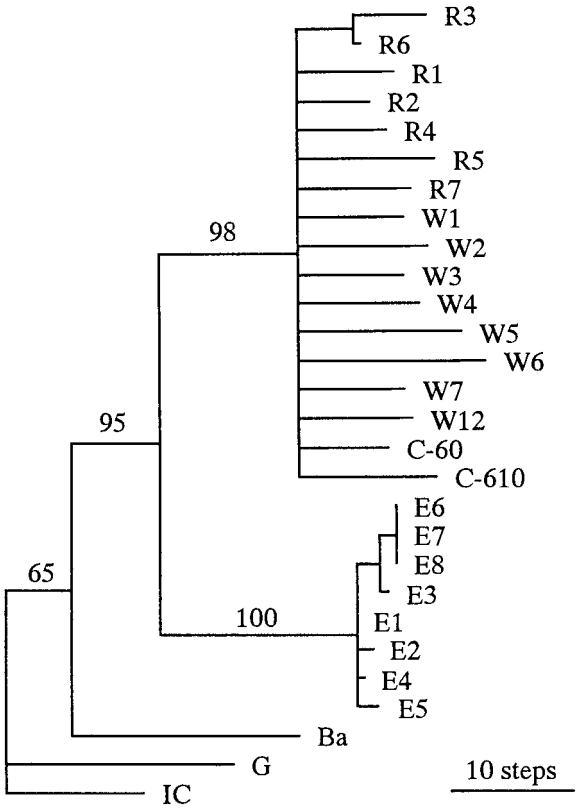

Figure 4. Phylogenetic tree of binucleate *Rhizoctonia* AG-D subgroups (I) and (II), AG-Ba and AG-G isolates. The tree length was 380 steps. Edges of length and bootstrap replication frequencies above 50% are indicated on the branches. A *Rhizoctonia solani* AG1-IC isolate was used as an outgroup to root the tree. For identification see Tables 2 and 3.

could anastomose with those of AG-D isolates, and they are now thought to belong to subgroup AG-D (I). A dendrogram constructed from the RAPD data also showed each of the two subgroups made an individual cluster with mean similarity coefficients of 0.62 for AG-D (I) and 0.94 for AG-D (II). The values of these two coefficients clearly show that the AG-D (I) group consists of variant isolates, while the AG-D (II) group consists of similar isolates. Although the isolates were acquired from various areas in Japan, the data of RFLP analysis of the ITS region from rDNA and of RAPD analysis obtained from subgroups AG-D (I) and AG-D (II) indicate that there are no geographical relationships among the isolates in these groups.

Based on RFLP analysis of the ITS region from rDNA and on RAPD analysis, isolates obtained from wheat exhibiting symptoms of foot-rot disease, and from mat rush with winter-stem-rot disease, belong to subgroup AG-D (I). These disease symptoms were found during the cool season in Japan (Ikata and Yoshida, 1940; Takamatsu, 1989), and the cultural characteristics and pathogenicity of these fungi are very similar to those of AG-D (I) isolates (Table 1). Thus, DNA analyses support the data for the season of occurrence, cultural characteristics, and pathogenicity for these isolates. Thus, we propose that isolates of foot-rot and winter-stem-rot diseases belong to subgroup AG-D (I).

In addition, CAG-1 isolates, causal agent of sharp-eye-spot of cereals, and of other diseases of several crop plants, were obtained during the cool season and their cultural characteristics were almost identical to subgroup AG-D (I) (Burpee, 1980; Lipps and Herr, 1982). Therefore, we also propose that the known CAG-1 isolates possibly belong to subgroup AG-D (I).

Subgroup AG-D (II) isolates causing elephant-footprint disease were clearly distinguished from AG-D (I) based on cultural characteristics, pathogenicity, and DNA analysis. Hyphae of all AG-D (II) isolates anastomosed with all AG-D (I) isolates. The results of RAPD analysis showed that the cluster composed of AG-D (II) isolates had high similarity, and that little variability was observed among the banding patterns of AG-D (II) isolates. So far, isolates belonging to subgroup AG-D (II) were not obtained from plants other than zoysiagrass. It would be interesting to know whether AG-D (II) isolates can be obtained only from warm-season turfgrasses, or if they occur more widely.

From these data, we conclude that AG-D should be divided into the two subgroups, AG-D (I) and (II), based on RFLP analysis of the ITS region from rDNA and on RAPD analysis.

Acknowledgements

We thank Cecilia B. Pascual, Drs. Fritz Tsao, Onwana-Agyeman Siaw and Terence McGonigle for critical reading of the manuscript.

References

Balali GR, Whisson DL, Scott ES and Neate SM (1996) DNA fingerprinting probe specific to isolates of *Rhizoctonia solani* AG-3. Mycological Research 100: 467–470

Boerma GH and Verhoeven AA (1997) Checklist for scientific names of common parasitic fungi. Series 26: Fungi on field crops: Cereals and grasses. Netherlands Journal of Plant Pathology 83: 165–204

Boysen M, Borja M, del Moral C, Salazar O and Rubio V (1996) Identification oat strain level of *Rhizoctonia solani* AG4 isolates by direct sequence of asymmetric PCR products of the ITS regions. Current Genetics 29: 174–181

Bruns TD, White TJ and Taylor JW (1991) Fungi molecular systematics. Annual Review of Ecology and Systematics 22: 525–564

Burpee LL (1980) *Rhizoctonia cerealis* yellow patch of turfgrass. Plant Disease 64: 1114–1116

Burpee LL, Sanders PL, Cole H and Sherwood RT (1980) Anastomosis groups among isolates of *Ceratobasidium cornigerum* and related fungi. Mycologia 72: 689–701

Carling DE and Leiner RH (1987) Categorization of anastomosis interactions that occur between isolates of *Rhizoctonia solani*. Phytopathology 77: 1777

Cubeta MA, Echandi E, Abernethy T and Vilgalys R (1991) Characterization of anastomosis groups of binucleate *Rhizoctonia* species using restriction analysis of an amplified ribosomal RNA gene. Phytopathology 81: 1395–1400

Damaj M, Jabaji-Hare SH and Charest PM (1993) Isozyme variation and genetic relatedness in binucleate *Rhizoctonia* species. Phytopathology 83: 864–871

Duncan S, Barton JE and O'Brien PA (1993) Analysis of variation in isolates of *Rhizoctonia solani* by random amplified polymorphic DNA assay. Mycological Research 97: 1075–1082

Hyakumachi M and Sumino A (1984) New morphological type (IC) in *Rhizoctonia solani* AG1 isolated from sugar beet manufactory waste soils and of its characteristics. Annals of the Phytopathological Society of Japan 50: 507–514

Ikata S and Yoshida M (1940) Studies on the disease of mat rush,1. Blight Special Bulletin, Okayama Agricultural Experiment Station 42: 1–47

Jabaji-Hare SH, Meller Y, Gill S and Charest PM (1990) Investigation of genetic relatedness among anastomosis groups of *Rhizoctonia solani* using cloned DNA probes. Canadian Journal of Plant Pathology 12: 393–404

Kataria HR and Hoffmann GM (1988) A critical review of plant pathogenic species of *Ceratobasidium* Rogers. Journal of Plant Disease and Protection 95: 81–107

Keijer J, Houterman PM, Dullemans AM and Korsman MG (1996) Heterogeneity in electrophoretic karyotype within and between anastomosis groups of *Rhizoctonia solani*. Mycological Research 100: 789–797

Lipps PE and Herr LJ (1982) Etiology of *Rhizoctonia cerealis* in sharp eyespot of wheat. Mycological Research 100: 789–797

Liu ZL and Sinclair JB (1992) Genetic diversity of *Rhizoctonia solani* anastomosis group 2. Phytopathology 82: 778–787

Liu ZL and Sinclair JB (1993) Differentiation of intraspecific groups within anastomosis group 1 of *Rhizoctonia solani* using ribosomal DNA internal transcribed spacer and isozyme comparisons. Canadian Journal of Plant Pathology 15: 272–280

Liu ZL, Domier LL and Sinclair JB (1993) ISG-specific ribosomal DNA polymorphism of the *Rhizoctonia solani* species complex. Mycologia 85: 795–800

Liu ZL, Domier LL and Sinclair JB (1995) Polymorphism of genes coding for nuclear 18S rDNA indicates genetic distinctiveness of anastomosis group 10 from other groups in the *Rhizoctonia solani* species complex. Applied and Environmental Microbiology 61: 2659–2664

Matsuoka M. (1959) On the winter sheath blight of rush plants. Kyushu Agricultural Research 21: 158

Mazzola M, Wong TO and Cook RJ (1996) Virulence of *Rhizoctonia oryzae* and *R. solani* AG-8 on wheat and detection of *R. oryzae* in plant tissue by PCR. Phytopathology 86: 354–360

Ogoshi A, Oniki M, Araki T and Ui T (1983) Anastomosis groups of binucleate *Rhizoctonia* in Japan and North America and their perfect stages. Transactions of the Mycological Society of Japan 24: 79–87

Ogoshi A, Oniki M, Sakai R and Ui T (1979) Anastomosis grouping among isolates of binucleate *Rhizoctonia*. Transactions of the Mycological Society of Japan 20: 33–39

Ogoshi A (1976) Studies on the grouping of *Rhizoctonia solani* Kuhn with hyphal anastomosis and on the perfect stages of groups. Bulletin of National Institute of Agricultural Science Series C 30: 1–63

Oniki M, Kobayashi K, Araki T and Ogoshi A (1986a) A new disease of turf-grass caused by binucleate Rhizoctonia AG-Q. Annals of the Phytopathological Society of Japan 52: 850–953

Oniki M, Ogoshi A and Araki T (1986b) *Ceratobasidium strarie*, *C. cornigeum*, and *C. gramineum*, the teleomorph of the pathogenic binucleate *Rhizoctonia* fungi from gramineous plants. Transactions of Mycological Society of Japan 27: 147–158

Schneider JHM, Salazar O, Rubio V and Keijer J (1997) Identification of *Rhizoctonia solani* associated with field-grown tulips using ITS rDNA polymorphism and pectic zymograms. European Journal of Plant Pathology 103: 607–622

Sneath PA and Sokal RR (1973) Numerical Taxonomy: The Principles and Practice of Numerical Classification. W.H. Freeman, San Francisco

Swofford DL (1993) PAUP: Phylogenetic Analysis Using Parsimony, Version 3.1.1. Computer program distributed by the Illinois Natural History Survey. Campaingn, IL

Takamatsu S (1989) A new snow mold of wheat and barley caused by the foot rot fungus, *Ceratobasidium gramineum*. Annals of the Phytopathological Society of Japan 55: 233–237

Tanaka A, Kitabayashi H, Tani T and Ogoshi A (1994) A pathogen causing patch so-called 'elephant footprint' on zoysia grasses. Annals of the Phytopathological Society of Japan (Abstr. and Japanese) 60: 344

Tani T (1989) Soil diseases of turfgrass. Noyaku Graph (Japanese) 109: 2–5

Tanpo H, Kudo J, Tani T and Ogoshi A (1990) The *Rhizoctonia* disease of bentgrass turf occurred in winter season in Japan. Journal Japanese Society of Turfgrass Science 19: 31–38

Uchino H, Kanazawa K and Ogoshi A (1983) Anastomosis group of binucleate *Rhizoctonia* isolated from diseased sugar beet seedlings. Memoirs of the Faculty of Agriculture Hokkaido University 13: 494–499

Vilgalys R and Gonzalez D (1990) Ribosomal DNA restriction fragment length polymorphism in *Rhizoctonia solani*. Phytopathology 80: 151–158

White TJ, Burns T, Lee S and Taylor J (1990) Amplification of PCR Products: A Guide to Methods and Applications. In: Innis MA, Gelfland DH, Sninsky JJ and White TJ (eds) (pp 315–321). Academic Press, San Diego, CA, USA

Yang J and Kharbanda PD (1996) Characterization, virulence and genetic variation of *Rhizoctonia solani* AG-9 in Alberta. Plant Disease 80: 513–518

Yap IV and Nilson RJ (1996) Winboot: A program for performing boot strap analysis of binary data to determine the confidence limits of UPGMA-based dendrograms. IRRI Discussion Paper Series No. 14. International Rice Research Institute, Manila, Philipinnes. 22 pp

Yoder OC (1988) *Cochliobolus heterostrophus* cause of southern corn leaf blight. In: Sidhu GS (ed) Advances in Plant Pathology, Vol 6 (pp 93–122). Genetics of Plant Pathogenic Fungi. Academic Press, London